CHARACTERIZING DIFFERENCES AMONG AUTOMATED AVALANCHE TERRAIN MAPPING APPROACHES: A MULTI-INSTITUTION COMPARISON AT ROGERS PASS, CANADA

John Sykes[1*], Stephan Harvey[2], Paula Spannring[3], Christoph Hesselbach[3], Kalin Markov[4], Pascal Haegeli[1,2], and Grant Statham[5]

[1]*Simon Fraser University Avalanche Research Program, Burnaby, BC, Canada*
[2]*WSL Institute for Snow and Avalanche Research SLF, Davos, Switzerland*
[3]*Austrian Research Centre for Forests, Department for Natural Hazards, Innsbruck, Austria*
[4]*National Institute of Geophysics, Geodesy and Geography, Bulgarian Academy of Sciences, Sofia, Bulgaria*
[5]*Parks Canada, Banff, AB, Canada*

ABSTRACT: Automated avalanche terrain mapping has become an established approach for communicating avalanche terrain exposure to public and professional backcountry users. Several groups have developed automated workflows that implement the Avalanche Terrain Exposure Scale (ATES) framework at scale by identifying start zones, simulating runouts, and assigning ATES classes. These approaches share the same class definitions but differ in how they parameterize release areas, represent forest, and translate terrain and avalanche characteristics into class ratings. This study compares four automated implementations at Connaught Creek in Rogers Pass, British Columbia, Canada. All products were generated on shared 5 m elevation and forest-cover data and compared against an ATES map produced manually and independently by three experts. Six avalanches from a high-magnitude rain-on-snow cycle, mapped by the local forecast team, provide an independent reference for the runout layers. All products show moderate to strong ordinal agreement with the expert map (quadratic-weighted kappa 0.59–0.73, which treats adjacent-class disagreements as less severe than distant ones); most differences are a single ATES class. The products differ more in the direction of disagreement than in its magnitude, reflecting the slope angle at which each escalates ratings and whether forest is used to reduce ratings. Release areas diverge most below 30°; runout layers are more similar, with typical-magnitude layers reaching 70–79 % of the mapped valley-bottom avalanches and larger-magnitude layers reaching 90–98 %. The closest automated product matches the level of agreement among the independent mappers themselves (exact agreement 65 % versus 63 %, weighted kappa 0.73 versus 0.71). The differences between each group's map outputs are modeling choices shaped by regional snow climate and design philosophy, not errors in applying a shared ATES framework. The comparison does not rank the products; it clarifies the trade-offs so that shared, flexible workflows can support regionally appropriate maps while drawing on collective institutional knowledge.

KEYWORDS: Automated avalanche terrain mapping; Avalanche Terrain Exposure Scale (ATES); runout simulation; model comparison

1. INTRODUCTION

The Avalanche Terrain Exposure Scale (ATES) classifies mountainous terrain based on the degree of exposure to avalanche hazard (Statham and Campbell 2025). The intent of ATES is to improve backcountry recreationists' ability to make informed risk management decisions during route planning by simplifying their terrain analysis. In practice, producing an ATES map has typically required an expert to delineate polygons or trail segments by hand. That process is time- and cost-intensive, so high-quality manual maps exist for only a small number of high-use areas. Manual ATES mapping is also inherently subjective, as it relies on local expertise to weigh the various factors in the ATES technical model and the public-facing communication model.

Several research institutions have responded by automating the mapping workflow, including the WSL Institute for Snow and Avalanche Research (SLF), the Austrian Research Centre for Forests (BFW), the Bulgarian Academy of Sciences (BAS), and the Simon Fraser University Avalanche Research Program (SFU).

White Risk (`https://whiterisk.ch`), the Swiss avalanche-prevention platform from SLF, pioneered delivering automated avalanche terrain maps to the public. Those maps include (1) Classified Avalanche Terrain (CAT), which shows potential release areas (PRA) and runout zones calculated from RAMMS for size class 3 avalanches; (2) Avalanche Terrain Hazard (ATH), a continuous hazard surface, considering release potential and consequences; (3) Classified Avalanche Terrain Hazard (ATHc), which recasts the same workflow onto an ATES-like scale (Harvey et al.

** Corresponding author address:*
John Sykes (presenting author), Simon Fraser University Avalanche Research Program,
Burnaby, BC, Canada; email: john_sykes@sfu.ca

https://doi.org/10.15788/1790098425

2024). These maps are primarily intended for scenarios which can occur every 2 to 10 years, they are not meant for extreme scenarios. Whereas the CAT and ATH map are available for the public in Switzerland, France and Austria, the ATHc map is not. The concept of the ATHc map is to assign the existing intermediate results from the various calculations and simulations, to the corresponding ATES classes, based on the ATES technical model.

The other three products share the same basic release–runout–classification structure but differ in important internal details. BFW adapted autoATES v2.0 to the terrain of the Austrian Alps by calibrating sub-models against reference data, tuning forest friction, and adjusting avalanche-size parameterizations (Hesselbach et al. 2026). BAS retained the same overall workflow but replaced the rule-based autoATES v2.0 classifier with a machine-learning model trained on expert-delineated data from a small part of the Pirin Mountains (Markov et al. 2025). The ML model generalized well to the rest of the range and has the practical advantage that it does not require extensive local tuning of rules and thresholds. SFU has continued the autoATES line: version 2.10 remains close to the original autoATESv2.0 framework (Toft et al. 2024), while version 3.0 rewrites the classification step and modifies both the PRA and runout methods (Sykes et al. 2026). In each case the customizations reflect local knowledge and are designed to fit the characteristics of the target terrain.

Although the products use the same ATES class definitions, differences in how the technical criteria are implemented can lead to differences in how the terrain is classified in the automated ATES maps. Spannring (2024) compared autoATES and SLF CAT, the release-and-runout layer, not the ATES-class ATHc map used here, at Davos and Sellrain and found that Simple aligned with CAT non-avalanche terrain and Extreme with CAT slopes steeper than 50°, while Challenging and Complex were mixed; runout-model choice (AvaFrame::com4FlowPy versus RAMMS::Extended) was a main source of the mismatch. Sykes et al. (2022) adapted the SLF PRA method in a Canadian study area in the Selkirk Mountains by lowering the slope floor and including forested start zones to better match local expert knowledge. The finished multi-agency ATES products have not been run together on a single North American study area, or scored against an expert ATES map and observed events. This matters because the maps are easily treated as interchangeable, and users may assume that class labels such as Challenging denote the same quantity in every product.

The objective of this paper is to compare automated avalanche terrain mapping approaches from four research institutions at Connaught Creek, Rogers Pass, Canada, against an ATES map produced by three experts. We first compare the resulting terrain classifications, and then examine release area delineation and runout extent. In addition we evaluate the runout layers against six observed avalanches. The aim is to locate where and on what terrain the models diverge, and why. This study does not aim to rank the models and, as we show below, model–expert agreement is already at the level at which the experts agree with each other.

2. METHODS

2.1. Study area

The comparison is conducted at Connaught Creek, a 13.0 km² drainage at Rogers Pass in the Selkirk Mountains of Glacier National Park, Canada. The valley floor sits near 1,300 m and the ridges reach approximately 2,700 m. Avalanche paths from both sidewalls run into the same creek, creating frequent overhead exposure. Parks Canada forecasts the area and maintains a long-standing avalanche control program for the Trans-Canada Highway and the Canadian Pacific Railway. The snow climate is transitional with a strong maritime influence (Shandro and Haegeli 2018). The most important persistent weak layers are facet–crust combinations, which typically form after early-season rain-on-snow events, and surface hoar. These layers produce start zones of slopes below 30° (Atkins et al. 2026; Sykes et al. 2022).

2.2. Expert reference map

Three experienced ATES mappers independently mapped the study area and then collaborated to produce a consensus map (Sykes et al. 2024). The mapping methods included field visits, desktop interpretation of satellite imagery and slope angles, and consultation with local experts; each mapper followed their own established practices for the independent maps. We use the consensus map as a common reference point rather than as ground truth. No automated product was designed to reproduce it. Note that the SFU autoATES v2.10 product shares methodological lineage with the reference.

Over the 13.06 km² covered by all three mappers, they agree on 63.1% of cells (weighted kappa =

0.71). We treat this level of agreement as the noise floor of the reference and return to it in the Discussion. One of the three mappers did not use a non-avalanche class anywhere in the study area.

2.3. Model inputs and products

All products were generated on shared 5 m elevation and forest-cover data derived from 1 m LiDAR and Sentinel-2 canopy cover. SLF treats dense forest as a mask: no PRA are delineated and no RAMMS simulations are started inside forest. BFW, BAS, and SFU incorporate forest canopy cover into the PRA model, runout friction and detrainment, and the ATES classifier.

SLF provided Classified Avalanche Terrain (CAT) and the corresponding ATHc classification for three design scenarios (2-, 10-, and 30-year return periods). We use the 30-year ATHc product for the ATES classification comparison and retain all three return-period runout layers for the runout evaluation. BFW supplied a 10 m product in two variants that share the same start-zone layer but differ in design-avalanche size. We use the maximum potential avalanche variant for the ATES classification comparison and retain both variants for the runout evaluation.

The SFU v3.0 entry is a development version described in a companion paper (Sykes et al. 2026); we treat it as a fifth product alongside SLF, BFW, BAS, and SFU v2.10. Its classification parameters were fitted on eight other Western Canada benchmark sites, with Connaught Creek held out so the comparison is independent. The main differences between SFU v2.10 and v3.0 are the addition of multiple PRA and runout scenarios that capture different magnitude events. Output layers from both the typical and infrequent scenarios are used in the ATES classification step to better match the characteristics of the ATES v2.0 technical model classes.

2.4. Observed avalanches

Six avalanches mapped by the Glacier National Park Mountain Safety Team during winter 2026 provide the only independent check on the runout layers (Figure 3b). All six occurred during a five-day rain-on-snow cycle from 16–20 March 2026 and are a convenience sample of high-magnitude, long-runout events rather than typical persistent-slab conditions. Mapped footprints range from 17.4 to 92.8 ha; inferred alpha angles range from 20.2° to 36.8° (median 30.5°). Some events stopped at the valley floor, so the observed range is limited by path geometry.

2.5. Comparison scale and metrics

We merge the non-avalanche class into Simple and compare all products on a four-class ordinal scale: Simple, Challenging, Complex, and Extreme. Distinguishing non-avalanche from Simple lies outside the design intent of most of these models. The BAS and BFW products contain no non-avalanche class; for SLF it mainly marks terrain outside modeled release and runout. Weighted kappa on this four-class scale is not directly comparable with five-class values reported in other studies.

ATES is ordinal, so our primary statistic is weighted kappa, which treats adjacent-class disagreements as less severe than distant ones. We also report exact percent agreement and mean directional bias relative to the expert map. For start-zone and runout layers we use intersection-over-union (IoU). Against the six mapped avalanches we report two one-sided scores: the share of the study area each runout layer flags, and the share of each mapped footprint it reaches.

3. RESULTS

3.1. ATES classification

This section reports how the products differ from the expert map and from one another (Figure 1). The maps show substantial overlap in the location of major start zones, avalanche paths, and valley-floor runout. The primary differences appear in where class boundaries are drawn and in how terrain near the edges of those distributions is assigned.

All five products achieve moderate to strong ordinal agreement with the expert map, with weighted kappa ranging from 0.59 to 0.73 and exact agreement from 47.9% to 65.3% (Table 1). Most disagreement consists of a single-class step. SFU v3.0 is closest to the expert map (65.3% exact agreement, weighted kappa 0.73), matching the level of agreement among the three experts themselves. Connaught Creek was held out during model fitting, so this performance is not the result of training on the reference map. SFU v2.10 follows (weighted kappa 0.69), consistent with its shared methodological lineage and with earlier western Canada validation results (Sykes et al. 2024).

The products differ more clearly in the direction of their disagreements than in overall agreement rates. BFW, SFU v2.10, and BAS assign a lower class than the experts on 34–37% of cells (for

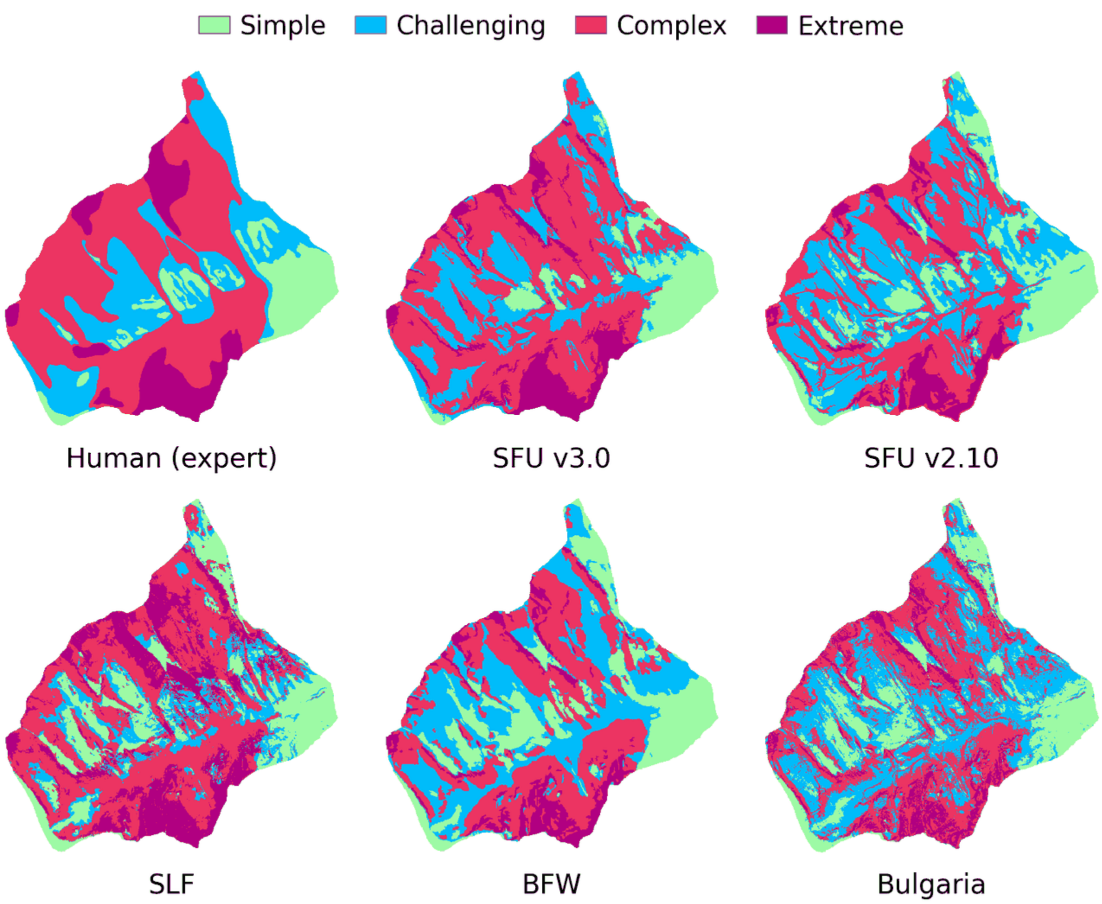

Figure 1: Expert and automated ATES maps.

Table 1: Four-class agreement with the expert consensus map. Bias and MAE in class units.

Product	***Exact (%)***	***Weighted kappa***	***Bias***	***MAE***	***Below expert (%)***
SLF ATHc (30-year)	54.8	0.642	$+0.055$	0.516	20.1
BFW (size 5)	52.2	0.648	-0.288	0.515	37.3
BAS (ML)	47.9	0.587	-0.248	0.570	37.0
SFU v2.10	57.7	0.691	-0.272	0.445	33.9
SFU v3.0	65.3	0.726	$+0.034$	0.364	16.1
Expert maps (noise floor)	63.1	0.714	—	—	—

example, Simple where the experts map Challenging). On average these three products rate approximately one-quarter to one-third of a class lower than the expert map. SLF rates slightly higher than the experts on average and assigns a lower class on only 20% of cells. SFU v3.0 shows little directional bias.

Figure 2b shows the slope-angle thresholds at which each product escalates class. The expert map assigns Complex at a median slope of 30.6° and Extreme at 46.2°. SLF is nearly identical (30.1° and 45.8°). BFW, BAS, and SFU v2.10 escalate later, at 35–36° for Complex and 51–53° for Extreme. SFU v3.0 falls between these groups for Complex (32–33°) and aligns with BFW, BAS, and SFU v2.10 for Extreme. The products therefore differ mainly in the slope angles at which they raise the ATES rating.

The products also diverge in their treatment of forest cover within the Simple and Challenging classes, then reconverge at higher classes (Figure 2c). Of the terrain the experts classify as Simple, 80% has canopy cover greater than 50%. The SFU products show similar or higher forest fractions. SLF, BAS, and BFW show lower fractions (40%, 39%, and 49%, respectively). Within the Challenging class the contrast is sharper: 40 % of SLF's terrain remains forested, compared with 8–20 % for the other products and 17 % for the experts. This difference follows directly from SLF's

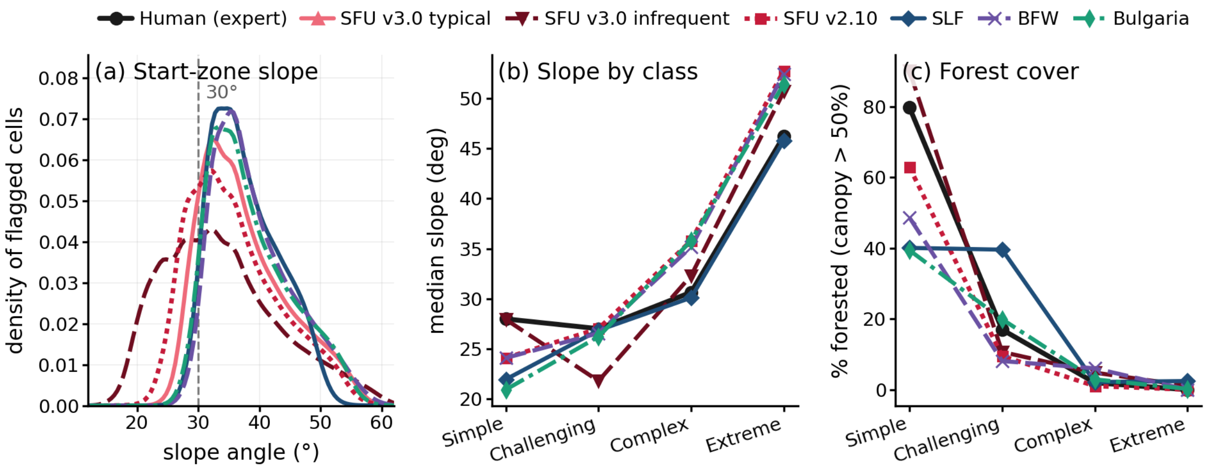

Figure 2: (a) Start-zone slope density, with SFU v3.0 shown as typical and infrequent release layers; (b) median slope by ATES class; (c) forest cover by ATES class.

approach of applying a pure slope-angle rule inside forest: 30–35° is classified as Simple (ATES 1), 35–45° as Challenging (ATES 2), and slopes steeper than 45° as Complex (ATES 3). The other products and the expert map more often place the same ground in Simple. Above Challenging the products agree closely: no more than 6% of Complex or Extreme terrain is forested in any product. Forest cover differs most among the products on the lower half of the ATES scale.

3.2. Start-zone extent and slope composition

PRA extent ranges from 3.6 km² for BFW (28 % of the valley) to 9.5 km² for the SFU v3.0 infrequent scenario (73 %). Between these extremes, SLF covers 4.5 km², BAS covers 4.8 km², the SFU v3.0 typical layer covers 5.5 km² (43 %), and SFU v2.10 covers 6.7 km² (52 %).

Nearly all of the difference occurs below 30° slope angle. SFU v2.10 flags 64 % of the 25–28° slope band and 81 % of the 28–30° band. SLF, BFW, and BAS flag only 1–4 % and 9–21 % of the same bands. As a result, approximately one-quarter of the SFU v2.10 start-zone area lies below 30°, compared with 3–5 % for SLF, BFW, and BAS. The SFU v3.0 typical layer sits between those groups (13 % below 30°); the infrequent layer puts 39 % of its start-zone area below 30°. In the BAS model this lower limit is explicit: the slope function, inherited from Veitinger et al. (2016), operates only between 28° and 60° and assigns a PRA value of zero outside that range. Figure 2a shows that SLF, BFW, and BAS terminate near a hard edge at approximately 30°, while the SFU v3.0 typical layer has a modest left shoulder below 30°, SFU v2.10 extends to about 25°, and the SFU v3.0 infrequent scenario reaches approximately 15°.

Despite these differences in extent, the products identify the same broad terrain features and differ mainly at the boundaries (Figure 3a). BAS and SLF are the most similar pair (IoU = 0.83). SFU v3.0 typical is also closely aligned with BAS (0.78) and SLF (0.70), and is the most similar of all products to SFU v2.10 (0.80). The SFU v3.0 infrequent layer is substantially less similar to the other agencies (IoU 0.38–0.50) because of its expanded low-angle footprint; its overlap with SFU v2.10 remains higher (0.71). Overall, SFU v2.10 and the infrequent scenario of v3.0 stand apart from the tighter cluster formed by SLF, BFW, BAS, and SFU v3.0 typical.

The large low-angle footprint of SFU v2.10 and the SFU v3.0 infrequent scenario is uncalibrated. Their slope-angle functions were fitted on coarser elevation data and applied to the 5 m LiDAR without retuning, so the extent of the low-angle reach is largely an artifact of that resolution transfer.

3.3. Runout extent and observed avalanches

Runout extent largely follows start-zone extent (Table 2). The smallest footprints belong to the typical-magnitude layers (SFU v3.0 typical 7.8 km², BFW size 3 8.0 km²); the largest belong to the infrequent and long-return-period layers (SFU v3.0 infrequent 11.2 km², SFU v2.10 10.7 km²). SLF spans 9.1–10.3 km² across its return-period scenarios, BAS covers 10.2 km², and BFW size 5 covers 9.2 km².

Pairwise spatial overlap among the runout layers is substantially higher and more uniform than among

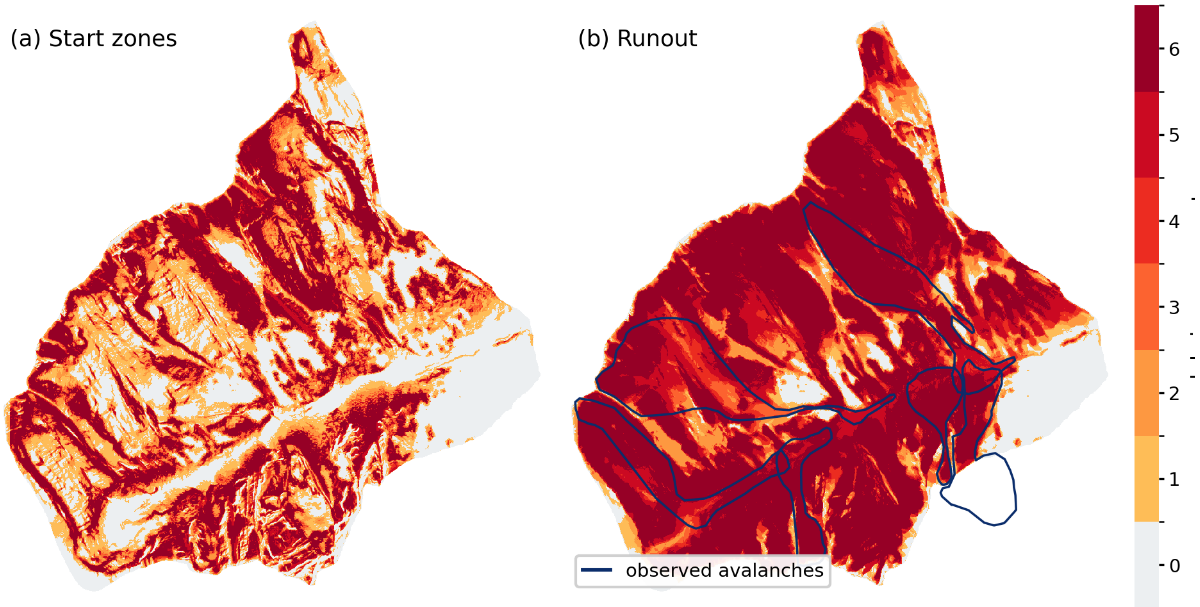

Figure 3: Number of six layers flagging each cell. (a) Start zones and (b) runout: SLF, BFW, BAS, SFU v2.10, SFU v3.0 typical and infrequent. Outlines in (b) are the six observed avalanches.

Table 2: Runout extent (% area of the study area) and coverage of the six mapped avalanches (% events). Typical-magnitude layers are shown for context.

Layer	***Area (km²)***	***% area***	***% events***
SLF 2-year	9.1	70.0	78.8
SLF 10-year	9.5	73.1	85.9
SLF 30-year	10.3	79.4	96.5
BFW size 3	8.0	61.6	72.9
BFW size 5	9.2	70.4	89.7
BAS	10.2	78.6	90.8
SFU v2.10	10.7	82.1	97.7
SFU v3.0 typical	7.8	60.0	69.7
SFU v3.0 infrequent	11.2	85.8	98.1

the start-zone layers (Figure 3b). All runout IoU values fall between 0.70 and 0.96. Once the models leave the start zones, the simulated deposits converge toward the same valley-bottom and gully-floor patterns regardless of differences in release-area parameterization.

Six avalanches mapped by the Glacier National Park forecast team during the March 2026 rain-on-snow cycle provide an independent check on these layers (Figure 3b). The events are a generally high-magnitude, estimated D3 to D4.5, long runout distance sample that represent unusually large avalanches for the area. The typical-magnitude layers (SLF 2-year, BFW size 3, SFU v3.0 typical) reach 70–79 % of the mapped footprints, while the larger-magnitude layers reach 90–98 % (Table 2).

4. DISCUSSION

4.1. Implications for map use

When two automated ATES maps of the same place are compared, agreement is expected on steep, open start zones, with the largest differences on forested moderate-angle slopes and on terrain between about 25° and 30°. In the runout zones the maps align much more closely; remaining differences are driven mainly by total runout distance, which depends on model parameterization. Overall, the spatial pattern of runout coverage is similar across products.

These disagreements are usually modeling choices rather than defects. The more useful question is which choice matches the snowpack of the region and the decision the map is intended to support. Automated ATES models are built around the technical model (Statham and Campbell 2025) and therefore reflect regional parameterization. Map users, however, primarily rely on the simpler ATES communication model to understand exposure. Regional adaptations that improve the fit to local conditions can still communicate overall exposure effectively through that simplified model, even when the underlying technical implementations are not identical. In practice these maps work best when combined with route-planning tools that describe cumulative exposure along a route or trail.

4.2. Modeling choices: low-angle release and multiple magnitude scenarios

Whether to include terrain below 30° is a design question, not something this comparison can settle. The parameterizations used by each group were chosen or calibrated for different mountain ranges and snow climates. In the Columbia Mountains, persistent weak layers (surface hoar and facet–crust combinations) commonly produce start zones on moderate slopes. Expert-mapped start zones in a nearby range sit well below 30° (Atkins et al. 2026; Sykes et al. 2022). A hard floor near 30° will miss that terrain by design.

The products make different choices on how to capture start zones (Figure 2a). SLF, BFW and BAS do not consider start zones below 30°. The SFU products reach farther for two reasons. First, both SFU v2.10 and the v3.0 infrequent scenario are intentionally biased toward lower-angle slopes to improve detection of moderate-terrain start zones that are common under persistent weak layers, accepting a higher false-detection rate. Second, an additional low-angle fringe appears as an artifact of resolution transfer: the slope functions were calibrated primarily on 30 m DSM data and then applied to 5 m LiDAR without retuning. The v3.0 typical scenario shows this second effect most cleanly. It retains a broadly similar slope distribution to the other agencies but is modestly skewed lower. SFU v2.10 combines both effects and places roughly a quarter of its start-zone area below 30°.

A parallel design choice appears in the runout layers. A single runout scenario cannot represent the full frequency–magnitude range in the ATES v2 technical model. Mapping Simple and non-avalanche terrain requires a large-magnitude layer; Table 2 shows that typical-magnitude layers miss many of the furthest-running March 2026 events. Using only the large layer expands Challenging and Complex too far down the path. SFU v3.0 therefore places both typical and infrequent start-zone and runout layers into the same classifier so each ATES threshold can draw on the scenario that fits best.

SLF, BFW and SFU encode the typical-versus-large split in different units (return interval, avalanche size, and a two-layer envelope). These are the same design job expressed in different quantities. How the scenarios are defined is a regional choice, driven by local snowpack and runout characteristics as well as the intended communication strategy with public users.

4.3. Comparing human and automated ATES maps

SFU v3.0 reaches the same level of agreement with the expert consensus map as the three independent mappers reach with one another (exact agreement 65 % versus 63 %, weighted kappa 0.73 versus 0.71). This is effectively the noise floor of the reference: further improvements against this particular consensus map would mostly reflect differences in mapping style rather than better terrain assessment. That limit does not mean every region needs a three-expert map. Those maps are time- and cost-intensive and are rarely available outside a few Canadian sites.

A more transferable path, and the one used in the autoATESv3.0 development, is to start from an automated map and have local experts edit where the model is wrong. That approach targets actual model error instead of differences among human mapping styles. Humans will not map at the resolution or precision of a digital elevation model; the automated map supplies that detail, and the expert pass supplies the local judgment. The companion paper develops this workflow for autoATES v3.0 and wall-to-wall mapping across western Canada (Sykes et al. 2026).

5. CONCLUSIONS

The comparison shows that automated avalanche terrain maps of the same place are not interchangeable, even when built on identical elevation and forest data. Start-zone layers diverge most below 30° and in forested moderate terrain. Runout layers are more similar; remaining differences are largely driven by design choices on whether to capture large-magnitude events. ATES classification inherits those differences and adds a further interpretive step, so the same class label can describe slightly different terrain depending on the product. Agreement is strongest in Complex and Extreme; the largest class-level differences occur in Simple and Challenging, where forest treatment and the low-angle release bound matter most. The technical implementations therefore diverge, yet the simpler ATES communication model still leaves room for regionally tuned maps to convey overall exposure. These offsets are modeling choices, not errors.

The choices themselves reflect different design philosophies. Capturing the full envelope of possible start zones and runouts requires conservative parameterization of slope angle and runout distance. Agencies willing to treat extreme events as outside the intended scope of a public map can stop closer to the typical end of the distribution. That decision is shaped by regional snow climate, by the intended user, and potentially by broader expectations about whether every hazard must be labeled or whether responsibility for residual risk rests with the end user.

The practical value of the comparison is therefore not a ranking but a clearer view of the trade-offs. Matching typical and infrequent design scenarios to local snow climate and runout potential produces maps that remain useful even when the underlying technical implementations differ. In regions where expert ATES maps are scarce and local mapping capacity is limited, the path to building reference data is to start from an automated product and use targeted expert review where the model diverges from local knowledge. Looking forward, the strongest gains will come from shared, flexible workflows that let each region calibrate start-zone and runout scenarios to its own conditions while still drawing on the collective knowledge of multiple institutions. Treating these models as a common infrastructure rather than competing products is the route to maps that are both locally appropriate and internationally coherent.

ACKNOWLEDGEMENTS

We thank Parks Canada for access to elevation data and the Glacier National Park Mountain Safety Team for mapping the six avalanches used as reference. We are grateful to the three ATES mappers who provided the Connaught Creek reference map. Financial support for this study was provided by Public Safety Canada through the Search and Rescue New Initiatives Fund (SARNIF) grant “Large-scale avalanche terrain exposure scale mapping for mountainous regions in Canada”. K. Markov acknowledges support from “AvalForCE,” funded by the MAPS program of the Swiss National Science Foundation and the Bulgarian Ministry of Education (grant IZ11Z0_230113).

REFERENCES

Atkins, R., Rigby, N., and Haegeli, P. (2026). A closer look at slope angles of accidentally triggered persistent and deep persistent slab avalanches. In: Proceedings of the International Snow Science Workshop. Whistler, Canada.

Harvey, S., Christen, M., Bühler, Y., Hänni, C., Boos, N., and Bernegger, B. (2024). Refined Swiss avalanche terrain mapping CATv2 / ATHv2. In: Proceedings of the International Snow Science Workshop.

Hesselbach, C., Spannring, P., Huber, A., and Fischer, J.-T. (2026). OpenNHM/AvalancheTerrainIdentification: Avalanche Terrain Identification. https://doi.org/10.5281/zenodo.22049056.

Markov, K., Huber, A., Panayotov, M., Hesselbach, C., Spannring, P., Fischer, J.-T., and Teich, M. (2025). Machine learning for automated avalanche terrain exposure scale (ATES) classification. In: Nat. Hazards Earth Syst. Sci. 25, pp. 4375–4403. https://doi.org/10.5194/nhess-25-4375-2025.

Shandro, B. and Haegeli, P. (2018). Characterizing the nature and variability of avalanche hazard in western Canada. In: Nat. Hazards Earth Syst. Sci. 18, pp. 1141–1158. https://doi.org/10.5194/nhess-18-1141-2018.

Spannring, P. (2024). Comparison of two avalanche terrain classification approaches: Avalanche Terrain Exposure scale – Classified Avalanche Terrain. thesis.

Statham, G. and Campbell, C. (2025). The Avalanche Terrain Exposure Scale (ATES) v.2. In: Nat. Hazards Earth Syst. Sci. 25, pp. 1113–1137. https://doi.org/10.5194/nhess-25-1113-2025.

Sykes, J., Haegeli, P., and Bühler, Y. (2022). Automated snow avalanche release area delineation in data-sparse, remote, and forested regions. In: Nat. Hazards Earth Syst. Sci. 22, pp. 3247–3270. https://doi.org/10.5194/nhess-22-3247-2022.

Sykes, J., Knies, D., Haegeli, P., and Anthony-Malone, K. (2026). AutoATES v3.0: automated ATES mapping at scale across western Canada. In: Proceedings of the International Snow Science Workshop. Whistler, Canada.

Sykes, J., Toft, H., Haegeli, P., and Statham, G. (2024). Automated Avalanche Terrain Exposure Scale (ATES) mapping – local validation and optimization in western Canada. In: Nat. Hazards Earth Syst. Sci. 24, pp. 947–971. https://doi.org/10.5194/nhess-24-947-2024.

Toft, H. B., Sykes, J., Schauer, A., Hendrikx, J., and Hetland, A. (2024). AutoATES v2.0: Automated Avalanche Terrain Exposure Scale mapping. In: Nat. Hazards Earth Syst. Sci. 24, pp. 1779–1793. https://doi.org/10.5194/nhess-24-1779-2024.

Veitinger, J., Purves, R. S., and Sovilla, B. (2016). Potential slab avalanche release area identification from estimated winter terrain: a multi-scale, fuzzy logic approach. In: Nat. Hazards Earth Syst. Sci. 16, pp. 2211–2225. https://doi.org/10.5194/nhess-16-2211-2016.